Thesis Title

Thesis Subtitle

Nathan Frederick Smith

A thesis presented in partial fulfillment of the degree of
Master's of Science

Department of Physics
McGill University, Montreal
Canada
??-??-2017

Dedication

Dedication here...

Acknowledgements

Acknowledgements here...

Abstract

English abstract...

Abrégé

French abstract...

Contents

List of Figures

List of Tables

Chapter 1

Introduction

- Foundation of material science is that microstructure influences properties
- We're not good at predicting microstructure
- We're getting better at it
- Look at these improvements

Chapter 2

Introduction to Classical Density Functional Theory

Many physical theories are derived using a succession of approximations. The utility of this approach is that, while each approximation yields a new theory that is more narrow in scope, the subsequent theory is typically more tractible to either analytical or numerical analysis. Classical Density Functional Theory (CDFT) is derived using this approach and in this chapter we'll examine each approximation and the intermediate theory they supply. In the following chapter, we'll see how CDFT can be used to examine the problem of solidification and how we can derive a more simplified theory, the Phase Field Crystal theory, from it.

CDFT is a theory of statistical mechanics. This means CDFT connects microscopic physics to macroscopic observables using statistical inference[1] instead of attempting to compute microscopic equations of motion. The microscopic physics in this case is most accurately described by many-body quantum mechanics and so the theory of quantum statistical mechanics is a natural starting point in any attempt to calculate thermodynamic observables.

We will see that for our systems of interest that the full quantum statistical theory is completely intractible. To preceed, we'll look at quantum statistical mechanics in the *semi-*

[1]Statistical mechanics is not always described as statistical inference. See works of E. T. Jaynes for details on this approach [8]

classical limit. In the semi-classical limit we'll develop a theory of inhomogenous fluids called Classical Density Functional Theory (CDFT). Finally, we'll see that constructing exactly free energy functionals for CDFT is rarely possible and look at an approximation scheme for these functionals.

2.1 Statistical Mechanics in the Semi-classical limit

Although the quantum statistical mechanics picture gives us a link between the microscopic and macroscopic reality of thermodynamics systems, it still contains too much detail. For instance, the precise bosonic or fermionic nature of the particles in the system often has little consequence on the thermodynamic properties. We can ignore some of these quantum mechanical details by looking at statistical mechanics in the *semi-classical limit*.

For the sake of clarity, we'll look at a system of N identical particles in the canonical ensemble which is straight forward to generalize to multi-component systems and other ensembles. We start with the definition of the partition function for a system of many particles,

$$Z = \mathrm{Tr}\left[e^{-\beta\hat{H}}\right], \tag{2.1}$$

where, $\hat{H} = \frac{|\mathbf{p}|^2}{2m} + V(\mathbf{q})$ and $\mathbf{p} = (p_1, p_2, ...p_N)$ is the vector of particle momenta. $\mathbf{q}$ is similarly defined for the particle positions. Wigner [20],and, shortly after, Kirkwood [10] showed that the partition function could be expanded in powers of $\hbar$, facilitating the calculation of both a classical limit and quantum corrections to the partition function. Their method, the Wigner-Kirkwood expansion, involves evaluating the trace operation over a basis of plane wave solutions,

$$\mathcal{Z}(\beta) = \int \frac{\mathrm{d}\mathbf{q}\mathrm{d}\mathbf{p}}{(2\pi\hbar)^N} e^{-\frac{i\mathbf{p}\cdot\mathbf{q}}{\hbar}} e^{-\beta\hat{H}} e^{\frac{i\mathbf{p}\cdot\mathbf{q}}{\hbar}} = \int d\Gamma I(\mathbf{q},\mathbf{p}), \tag{2.2}$$

Where, $d\Gamma$ is the phase space measure $\mathrm{d}\mathbf{p}\mathrm{d}\mathbf{q}/(2\pi\hbar)^N$. To compute the integrand, $I(\mathbf{q},\mathbf{p})$, we

follow Uhlenbeck and Bethe [19] and first compute its derivative,

$$\frac{\partial I(\mathbf{q},\mathbf{p})}{\partial \beta} = -e^{\frac{i\mathbf{p}\cdot\mathbf{q}}{\hbar}} \hat{H} e^{-\frac{i\mathbf{p}\cdot\mathbf{q}}{\hbar}} I(\mathbf{q},\mathbf{p}). \tag{2.3}$$

If we then make a change of variables, $I(\mathbf{q},\mathbf{p}) = e^{-\beta\mathcal{H}} W(\mathbf{q},\mathbf{p})$, where $\mathcal{H}$ is the classical Hamiltonian, and use the explicit form of the quantum Hamiltonian we arrive at a partial differential equation for W.

$$\frac{\partial W}{\partial \beta} = \frac{\hbar^2}{2}\left(\nabla_{\mathbf{q}}^2 - \beta(\nabla_{\mathbf{q}}^2 V) + \beta^2(\nabla V)^2 - 2\beta(\nabla_{\mathbf{q}} V)\cdot\nabla_{\mathbf{q}} + 2\frac{i}{\hbar}\mathbf{p}\cdot(\nabla_{\mathbf{q}} - \beta\nabla_{\mathbf{q}})\right) W(\mathbf{q},\mathbf{p}) \tag{2.4}$$

The solution can be written as a power series in $\hbar$, $W = 1 + \hbar W_1 + \hbar W_2 + ...$ This creates a power series expansion for the partition function as well,

$$\mathcal{Z} = (1 + \hbar \langle W_1 \rangle + \hbar^2 \langle W_2 \rangle + ...) \int d\Gamma e^{\beta\mathcal{H}}. \tag{2.5}$$

Where the average, $\langle\cdot\rangle$, denotes the the classical average,

$$\langle A(p,q) \rangle = \frac{1}{\mathcal{Z}} \int d\Gamma A(p,q) e^{-\beta\mathcal{H}}. \tag{2.6}$$

For the sake of brevity we'll quote solution to second order, but details can be found in Landau and Lifshitz [12].

$$\langle W_1 \rangle = 0 \tag{2.7}$$

$$\langle W_2 \rangle = -\frac{\beta^3}{24m} \left\langle |\nabla_{\mathbf{q}} V|^2 \right\rangle \tag{2.8}$$

The first order term is zero, because $W_1(\mathbf{q},\mathbf{p})$ is an odd function of $\mathbf{p}$. In terms of the Helmholtz free energy, for example, the corrections to second order would be,

$$\mathcal{F} = \mathcal{F}_{classical} + \frac{\hbar^2\beta^2}{24m} \left\langle |\nabla_{\mathbf{q}} V(\mathbf{q})|^2 \right\rangle. \tag{2.9}$$

There are a few items of importance in equation 2.9. First of all the correction inversely proportional to both the temperature and the particle mass. For copper at room termperature, for instance, the prefactor $\hbar^2\beta^2/(24m)$ is $\mathcal{O}(10^{-4})$. The correction is also proportional to the mean of the squared force felt by each particle. So high density materials will have a higher quantum correction because they sample the short-range repulsive region of the pair potential more than their low density counter parts.

2.1.1 Indistinguishability

There is an important distinction to be made between the quantum theory and the theory in the semi-classical limit. The integral over phase space of the partition function must only take into account the *physically different* states of the system. In the quantum theory this is acheived by tracing over any orthonormal basis of the Hilbert space, but in the classical theory we need to be careful not to double count states when identical particles are in the theory. Exchange of two identical particles does not result in a physically different state and thus this state should only be considered only once in the sum over states in the partition function. More precisely, we should write the classical partition function as,

$$\mathcal{Z} = \int' d\Gamma e^{-\beta\mathcal{H}}, \tag{2.10}$$

Where the primed integral denotes integration only over the physically distinct states. In the common case of N identical particles, the phase space integral becomes,

$$\int' d\Gamma \to \frac{1}{N!}\int d\Gamma \tag{2.11}$$

Aggregating our results, we can write the partition function in the semi-classical limit as,

$$\mathcal{Z}(\beta) = \frac{1}{N!}\int d\Gamma e^{-\beta\mathcal{H}} + \mathcal{O}(\hbar^2), \tag{2.12}$$

Or, in the grand canonical ensemble,

$$\Xi(\mu,\beta) = \sum_{N=0}^{\infty} \frac{e^{\beta\mu N}}{N!} \int d\Gamma \left(e^{-\beta\mathcal{H}} + \mathcal{O}(\hbar^2) \right) \tag{2.13}$$

Of course, to first order in $\hbar$, this is exactly the form taught in introductory courses on statistical mechanics and derived by Gibbs[2] prior to any knowledge of quantum mechanics [4]. The key insight here is to understand, in a contolled way, when this approximation is accurate and the magnitude of the next quantum correction is as seen in equation 2.9.

2.2 Classical Density Functional Theory

Ostensibly, when we study formation and evolution of microstructure in solids, our observable of interest is the density field. As per usual in theories of statistical thermodynamics we must distinguish between microscopic operators and macroscopic observables (the later being the ensemble average of the former). In classical statistical mechanics, operators are simply functions over the phase space, Γ. We use the term operator to make connection with the quantum mechanical theory. In the case of the density field, the microscopic operator is the sum of Dirac delta functions at the position of each particle,

$$\hat{\rho}(x;\mathbf{q}) = \sum_{i=0}^{N} \delta^{(3)}\left(x - q_i\right) \tag{2.14}$$

From which the thermodynamic observable is,

$$\rho(x) = \langle \hat{\rho}(x;\mathbf{q}) \rangle = \mathrm{Tr}\left[\hat{\rho}(x;\mathbf{q}) f(\mathbf{q},\mathbf{p})\right] \tag{2.15}$$

[2]The $\hbar$ in Gibbs' formula was justified on dimensional grounds and was simply a scaling factor with units of action $(J \cdot s)$

Where, $\mathrm{Tr}\,[\cdot]$ denotes the classical trace[3],

$$\mathrm{Tr}\,[A(\mathbf{q},\mathbf{p})f(\mathbf{q},\mathbf{p})] = \sum_{N=0}^{\infty} \frac{1}{N!} \int \mathrm{d}\Gamma A(\mathbf{q},\mathbf{p})f(\mathbf{q},\mathbf{p}), \tag{2.16}$$

And, $f(\mathbf{q},\mathbf{p})$ is the probability density function,

$$f(\mathbf{q},\mathbf{p}) = \frac{e^{-\beta(\mathcal{H}-\mu N)}}{\Xi(\mu,\beta)}. \tag{2.17}$$

To construct a theory of the density field we review the usual methodology for statistical thermodynamics. We will do so in the frame of entropy maximization in which the entropy is maximized subject to the macroscopically available information. Taking the existance of a average of the density field, particle number and energy as the macroscopically available information, we can maximize the entropy functional,

$$S[f(\mathbf{q},\mathbf{p})] = -k_b \mathrm{Tr}\left[f(\mathbf{q},\mathbf{p}) \ln\left(f(\mathbf{q},\mathbf{p})\right)\right], \tag{2.18}$$

subject to the aforementioned contraints to find a probability density function of the form,

$$f(\mathbf{q},\mathbf{p}) \propto \exp\left(-\beta(\mathcal{H} - \mu N + \int \mathrm{d}x \phi(x)\hat{\rho}(x)\right). \tag{2.19}$$

Where, β, μ and $\phi(x)$ are the Lagrange multipliers associated with constraints of average energy, number of particles and density respectively. As you might imagine, the constraints of average particle number and density are not independent and with the insight that,

$$N = \int dx \hat{\rho}(x), \tag{2.20}$$

[3]The classical trace in the grand canonical example in this particular case

We can combine their Lagrange multipliers into one,

$$f(\mathbf{q},\mathbf{p}) \propto \exp\left(-\beta(\mathcal{H} - \int \mathrm{d}x\psi(x)\hat{\rho}(x))\right), \tag{2.21}$$

Where, $\psi(x) = \mu - \phi(x)$, is the combined Langrange multiplier named the *intrinsic chemical potential*. Recalling that chemical potential is the change Helmholtz free energy made by virtue of adding particles to the system,

$$\frac{\partial F}{\partial N} = \mu, \tag{2.22}$$

The interpretation of the intrinsic chemical potential follows as the Helmholtz free energy change due to particles being added to a specific location. We'll see this in more detail briefly. Now, as with all statistical mechanics theories, the challenge to is to compute the moment generating function (partition function) or equivalently the cumulant generating function (free energy) so as to compute the statistics of our observable of choice. In case of observables of the density field, this is made somewhat more technical by the fact that the density is an entire function instead of a scalar variable. As such the partition function is more precisely called the partition *functional* and the free energy function is more precisely called the free energy *functional*. Specifically, the grand canonical partition functional is,

$$\Xi[\psi(x)] = \mathrm{Tr}\left[\exp\left(-\beta\mathcal{H} + \beta\int \mathrm{d}x\psi(x)\hat{\rho}(x)\right)\right]. \tag{2.23}$$

As eluded to above, the partition function is a type of moment generating functional in that repeated functional differentiation yields moments of the density field:

$$\frac{\beta^{-n}}{\Xi}\frac{\delta^n\Xi[\psi]}{\delta\psi(x_1)\dots\delta\psi(x_n)} = \langle\hat{\rho}(x_1)\dots\hat{\rho}(x_n)\rangle\,. \tag{2.24}$$

Similarly, we can construct a free enery functional by taking the logarithm of the partition

function. This free energy functional in particular is called the *grand potential functional*.

$$\Omega[\psi(x)] = -k_b T \log\left(\Xi[\psi(r)]\right) \tag{2.25}$$

The grand potential functional is a type of cumulant generating functional in the sense that repeated functional differentiation yields cumulants of the density field:

$$-\frac{\beta^{-n+1}\delta^n \Omega[\psi]}{\delta\psi(x_1)\dots\delta\psi(x_n)} = \langle \hat{\rho}(x_1)\dots\hat{\rho}(x_n)\rangle_c \tag{2.26}$$

Where, $\langle A^1 \dots A^n\rangle_c$, denotes the n-variable joint cumuluant.

If we examine the first two cumulants,

$$-\frac{\delta\Omega[\psi]}{\delta\psi(x)} = \langle\hat{\rho}(x)\rangle \equiv \rho(x), \tag{2.27}$$

$$-k_b T\frac{\delta^2\Omega[\psi]}{\delta\psi(x)\delta\psi(x')} = \langle(\hat{\rho}(x)-\rho(x))(\hat{\rho}(x')-\rho(x'))\rangle\,, \tag{2.28}$$

We notice something remarkable: The first, implies that the average density field is a function of only its conjugate field, the intrinsic chemical potential, and the second implies that that relationship is invertible[4]. To see this, we compute the Jacobian by combining equation 2.27 and 2.28,

$$\frac{\delta\rho(x)}{\delta\psi(x')} = \beta\,\langle(\hat{\rho}(x)-\rho(x))(\hat{\rho}(x')-\rho(x'))\rangle\,. \tag{2.29}$$

The right hand side of equation 2.29 is an autocorrelation function and therefore positive semi-definite by Weiner-Khinchin theorem. This implies that, at least locally, the intrinsic chemical potential can always be written as a functional of the average density, $\psi[\rho(x)]$, and vice versa. Furthermore, because all of the higher order cumulants of the density depend on the intrinsic chemical potential, they too depend only on the average density.

[4]The inverse function theorem only implies local invertibility, there is no guarentee of global invertibility. Indeed phase coexistance is a manifestation of this fact where a single intrinsic chemical potential is shared by two phases

Given the importance of the average density, $\rho(x)$, if follows that we would like to use a thermodynamic potential with a natural dependence on the density. We can construct a generalization of the Helmholtz free energy that has precisely this characteristic by Legendre transforming the Grand potential,

$$\mathcal{F}[\rho(x)] = \Omega[\psi[\rho]] + \int dx \rho(x)\psi(x). \tag{2.30}$$

$\mathcal{F}[\rho(x)]$ is called the *intrinsic free energy functional*.

It can be shown [6] that $\rho(x)$ must be the global minimum of the grand potential, which sets the stage for the methodology of classical density functional theory: if we have a defined intrinsic free energy functional, $\mathcal{F}$, we can find the equilibrium density field by solving the asssociated Euler-Lagrange equation,

$$\frac{\delta\Omega[\rho]}{\delta\rho(r)} = 0. \tag{2.31}$$

2.3 Techniques in Density Functional Theory

The difficulty in formulating a density functional theory is the construction of an appropriate free energy functional. While exact calculations are rarely feasible, there are a variety of techniques that help in building approximate functionals. Its important to note first what we *can* compute exactly. In the case of the ideal gas, we can compute the grand potential and free energy functional exactly,

$$\Omega_{id}[\psi] = -\frac{k_b T}{\Lambda^3} \int \mathrm{d}x\, e^{\beta\psi(x)} \tag{2.32}$$

$$\mathcal{F}_{id}[\rho] = k_b T \int \mathrm{d}x \left\{ \rho(x) \ln\left(\Lambda^3 \rho(x)\right) - \rho(x) \right\}, \tag{2.33}$$

Where Λ is the thermal de Broglie wavelength,

$$\Lambda = \sqrt{\frac{h^2}{2\pi m k_b T}}. \tag{2.34}$$

We may then express a deviations from ideality by factoring the ideal contribution out of the partition function,

$$\Xi[\psi] = \Xi_{id}[\psi]\Xi_{ex}[\psi], \tag{2.35}$$

leading to grand potential and free energy functionals split into ideal and *excess* components,

$$\Omega = \Omega_{id} + \Omega_{ex} \tag{2.36}$$

$$\mathcal{F} = \mathcal{F}_{id} + \mathcal{F}_{ex}. \tag{2.37}$$

The interaction potential, $V(\mathbf{q})$, in the excess partition function typically makes a direct approach to calculating the excess free energy intractible. Though perturbative methods, including the cluster expansion technique [14], have been developed to treat the interaction potential systematically, other approximation schemes for the excess free energy are typically more pragmatic. In particular, we can approximate the excess free energy by expanding around a reference homogeneos fluid with chemical potential μ_0 and density ρ_0,

$$\mathcal{F}_{ex}[\rho] = \mathcal{F}_{ex}[\rho_0] + \left.\frac{\delta \mathcal{F}_{ex}}{\delta \rho(x)}\right|_{\rho_0} * \Delta\rho(x) + \frac{1}{2}\Delta\rho(x') * \left.\frac{\delta^2 \mathcal{F}_{ex}}{\delta\rho(x)\delta\rho(x')}\right|_{\rho_0} * \Delta\rho(x) + \ldots, \tag{2.38}$$

Where $\Delta\rho(x) = \rho(x) - \rho_0$ and we have introduced the notation, $*$ to mean integration over repeated co-ordinates,

$$f(x') * g(x') \equiv \int \mathrm{d}x' f(x')g(x'). \tag{2.39}$$

The excess free energy is the generating functional of family of correlation functions called

direct correlation functions,

$$\frac{\delta^n \mathcal{F}_{ex}[\rho]}{\delta\rho(x_1)...\delta\rho(x_n)} = -\beta C^n(x_1, \ldots, x_n). \tag{2.40}$$

The first of which, for a uniform fluid, is the excess contribution to the chemical potential which we may express as the total chemical potential less the ideal contribution,

$$\left.\frac{\delta F_{ex}}{\delta\rho}\right|_{\rho_0} = \mu_0^{ex} = \mu_0 - \mu_{id} = \mu_0 - k_b T \ln\left(\Lambda^3\rho_0\right). \tag{2.41}$$

Should we truncate the expansion in equation 2.38 to second order in $\Delta\rho(x)$ and substitute the linear and quadratic terms with equation 2.41 and 2.40 we can simplify the excess free energy to,

$$\mathcal{F}_{ex}[\rho(r)] = \mathcal{F}_{ex}[\rho_0] + \int dr \left\{\mu - k_b T \ln\left(\Lambda^3\rho_0\right)\right\} \Delta\rho(r) - \frac{k_b T}{2}\Delta\rho(r) * C_0^{(2)}(r, r') * \Delta\rho(r') \tag{2.42}$$

Combining equation 2.33 with the simplified excess free energy in equation 2.42, we can express total change in free energy, $\Delta\mathcal{F} = \mathcal{F} - \mathcal{F}[\rho_0]$, as,

$$\Delta\mathcal{F}[\rho(r)] = k_b T \int \mathrm{d}r \left\{\rho(r) \ln\left(\frac{\rho(r)}{\rho_0}\right) - (1 - \beta\mu_0)\Delta\rho(r)\right\} - \frac{k_b T}{2}\Delta\rho(r) * C_0^{(2)}(r, r') * \Delta\rho(r'). \tag{2.43}$$

We find an equivalent expression for the grand potential after a Legendre transform,

$$\Delta\Omega[\rho(r)] = k_b T \int \mathrm{d}r \left\{\rho(r) \left[\ln\left(\frac{\rho(r)}{\rho_0}\right) + \beta\phi(r)\right] - \Delta\rho(r)\right\} - \frac{k_b T}{2}\Delta\rho(r) * C_0^{(2)}(r, r') * \Delta\rho(r'). \tag{2.44}$$

Its reasonable to ask at this point whether or not we have really gained anything with this approximation scheme. Although we have arrived at a relatively simple form for the free energy functional, we've added a lot of parameters to the functional based on the reference fluid. Thankfully, the theory of homogeneous liquids, such as our reference liquid, is very

well established. This means we may relay on a broad choice of analytical, numerical or experimental techniques to derive these parameters.

Equation 2.43 establishes an approximate density functional theory for inhomogenous fluids and, as we will see in the following chapter, for the seemingly disparate phenonmena of solidification. We see that it can derived through a series of approximations from a fundamental basis in quantum statistical mechanics and requires no more parameters than the thermodynamic details of a homogeneous reference fluid.

Chapter 3

Classical Density Functional Theory of Freezing

The classical density functional theories derived in chapter 2 was first established to study inhomogenous fluids. By considering the solid state as an especially extreme case of an inhomogeneous fluid [7], we can use CDFT to study the process of solidification. From the perspective of CDFT, solidification occurs once the density field develops long range periodic solutions. While not expressed in precisely this language, this approach dates back as far as 1941 with the early work of Kirkwood and Monroe [11] and was later significantly refined by Youssof and Ramakrishnan [17].

We'll see that the approach of Youssof and Ramakrishnan was very successful at explaining the solidification in the thermodynamic sense. That is to say, it elucidate the parameters responsible for solidification but not the dynamical pathway responsible for the transition. To discuss the pathway to equilibrium and the non-equilibrium artifacts it introduces into many solids (grain boundaries, vacancies, dislocations etc) we proceed to extend the CDFT framework using the Dynamic Density Functional Theory (DDFT). Noting that the full DDFT framework can be cumbersome in practice we conclude by introducing a simplified density functional theory called the Phase Field Crystal (PFC) theory.

3.1 Amplitude Expansions

To explore the problem of solidification, we begin with the approximate grand potential established in equation 2.44 with the external potential, $\phi(r)$, set to zero,

$$\beta\Delta\Omega[\rho(r)] = \int dr \left\{ \rho(r) \ln\left(\frac{\rho(r)}{\rho_0}\right) - \Delta\rho(r) \right\} - \frac{1}{2}\Delta\rho(r) * C_0^{(2)}(r, r') * \Delta\rho(r'). \tag{3.1}$$

To make our theory concrete we must choose a suitable reference liquid to set the parameters ρ_0 and $C_0^{(2)}(r, r')$. We will choose the reference liquid to be the liquid at the melting point with density ρ_l.

Scaling out a factor of ρ_l we can rewrite the grand potential in terms of a dimensionless reduced density, $n(r) \equiv (\rho(x) - \rho_l)/\rho_l$,

$$\frac{\beta\Delta\Omega[n(r)]}{\rho_l} = \int dr \left\{ (1 + n(r)) \ln(1 + n(r)) - n(r) \right\} - \frac{1}{2} n(r) * \rho_l C_0^{(2)}(r, r') * n(r'). \tag{3.2}$$

To describe the density profile in the solid state we can expand the density in a plane waves,

$$n(r) = \bar{n} + \sum_{\mathbf{G}} \xi_{\mathbf{G}} e^{i\mathbf{G}r}. \tag{3.3}$$

Where, $\{\mathbf{G}\}$, is the set of reciprocal lattice vectors in the crystal lattice and the amplitudes, $\xi_{\mathbf{G}}$, serve as order parameters for freezing. In the liquid phase all amplitudes are zero and the average density is uniform, while in the solid phase there are finite amplitudes that describe the periodic profile of the crystal lattice. By design, $\bar{n}$ is zero for the liquid phase at the melting point and $\bar{n}$ is the fractional density change of solidification, η for the solid phase at the melting point. Where,

$$\eta = \frac{\rho_s - \rho_l}{\rho_l}, \tag{3.4}$$

In which ρ_s is the macroscopic density of the solid phase.

The amplitudes are constrained by the point group symmetry of the lattice. Grouping

the amplitudes of symmetry-equivalent reciprocal lattice vectors together we can write the density profile as,

$$n(r) = \bar{n} + \sum_{\alpha} \left\{ \xi_\alpha \sum_{\{\mathbf{G}\}_\alpha} e^{i\mathbf{G}\cdot\mathbf{x}} \right\}, \tag{3.5}$$

Where α is a label running over sets of symmetry-equivalent reciprocal lattice vectors.

If we insert equation 3.5 into equation 3.2 and integrate over the unit cell we find,

$$\begin{aligned} \frac{\beta\Delta\Omega_{cell}}{\rho_l} = & \int_{cell} dr \left\{ (n(r)+1)\ln(n(r)+1) - n(r) \right\} \\ & - \frac{1}{2}\left[\bar{n}^2 \rho_l \tilde{C}_0^{(2)}(0) + \sum_{\alpha} \rho_l \tilde{C}_0^{(2)}(\mathbf{G}_\alpha)\lambda_\alpha |\xi_\alpha|^2 \right], \end{aligned} \tag{3.6}$$

Where λ_α is the number of reciprocal lattice vectors in the set α and $\tilde{C}_0^{(2)}(k)$ is the Fourier transform of the direct correlation function of the reference fluid. The first term in equation 3.6 is convex in all of the amplitudes with a minimum at zero. It is noteworthy, as we will see discuss shortly, that the product $\rho_l \tilde{C}_0^{(2)}(\mathbf{G}_\alpha)$ is a simple function of the structure factor, $S(k)$[1] ,

$$\rho\tilde{C}(k) = \frac{S(k)-1}{S(k)} \quad \forall\ k \neq 0. \tag{3.7}$$

It follows that solidification must occur when the product $\rho_l \tilde{C}_0^{(2)}(\mathbf{G}_\alpha)$ (or equivalently, the reference structure factor $S_0(\mathbf{G}_\alpha)$) is large enough to stabilize a finite amplitude by creating a new minimum away from zero. This phenomena is shown schematically in figure 3.1 where the grand potential is projected on to a particular ξ_α axis and plotted for different values of the reference structure factor.

[1]This follows from the definition of the structure factor and the Ornstein-Zernike equation

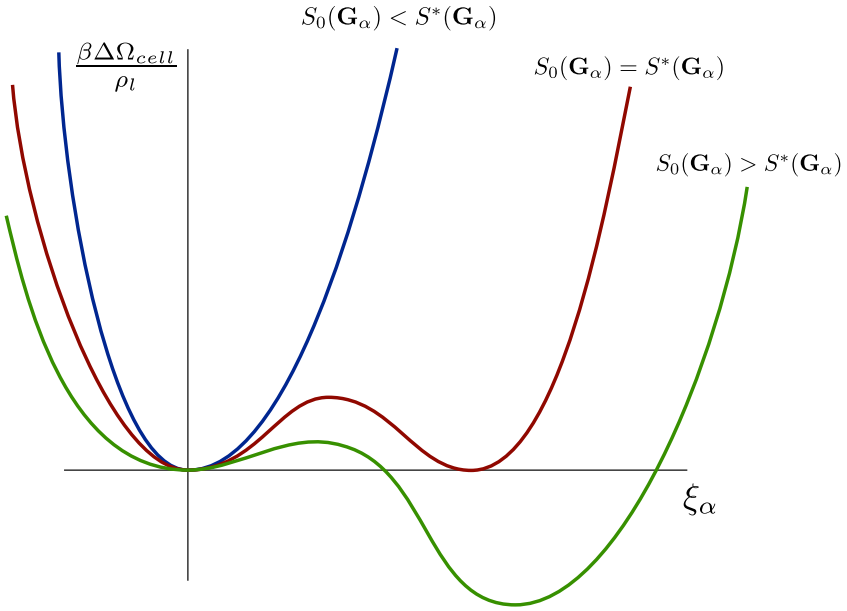

Figure 3.1: Schematic view of the grand potential $\beta\Delta\Omega/\rho_l$ projected on to the ξ_α axis for a three different reference structure factors. To minimize the grand potential, finite ξ_α is stable once $S_0(\mathbf{G}_\alpha) > S^*(\mathbf{G}_\alpha)$

Furthermore, equation 3.6 suggests that the set of critical structure factors, $\{S^*(\mathbf{G}_\alpha)\}_\alpha$ are material independent as no material dependent parameters remain in the grand potential. As a consequence, once we specify the symmetry of the lattice a liquid will solidify into (eg. face-centred-cubic), all materials that undergo this transition should share these parameters at the melting point.

This seems to be the case for a variety of materials. For instance, for many liquids solidifying into face-centred-cubic (fcc) lattices, these parameters for the [111] and [311] reciprocal lattice vectors are 0.65 and 0.23 respectively. Similarly, for a spectrum of liquids solidifying into body-centred-cubic (bcc) lattices these parameters for the [110] and [211] reciprocal lattice vectors are approximately 0.66 and 0.12 respectively.

As seen in table 3.1 and table 3.2 theoretical results from this approach match very closely to experimental values. In spite of the successes of density functional approach pioneered by Youssof and Ramakrishnan there are limits to this framework.

Many of the mechanical properties of solids are due to the way in which they deviate from

Theory	$\tilde{C}(\mathbf{G}_{[111]})$	$\tilde{C}(\mathbf{G}_{[311]})$	$\bar{n}$
I	0.95	0.0	0.074
II	0.65	0.23	0.270
III	0.65	0.23	0.166
Experiment	0.65	0.23	0.148

Table 3.1: Freezing parameters for Argon (fcc) taken from [17]. Theory I uses one order paramter, theory II uses two order parameters and theory III uses two order parameters and expands to third order in the free energy. η is the fractional density change of solidification $(\rho_s - \rho_l)/\rho_l)$.

Theory	$\tilde{C}(\mathbf{G}_{[110]})$	$\tilde{C}(\mathbf{G}_{[211]})$	$\bar{n}$
I	0.69	0.00	0.048
II	0.63	0.07	0.052
III	0.67	0.13	0.029
Experiment	0.65	0.23	0.148

Table 3.2: Freezing parameters for Sodium (bcc) taken from [17]. Theory I uses one order paramter, theory II uses two order parameters and theory III uses two order parameters and expands to third order in the free energy. η is the fractional density change of solidification $(\rho_s - \rho_l)/\rho_l)$.

the perfect crystalline lattice: the microstructure. Grain boundaries, vacancies, dislocations and second phase particles all play critical roles in determining the mechanical properties of solids. A simple example of this is the Hall-Petch effect which states that the yield stress of a material increases with decreasing grain size,

$$\sigma = \sigma_0 + k_y d^{-1/2}, \tag{3.8}$$

where, d, is the average grain diameter, σ is the yield stress, σ_0 is yield stress of a single crystal sample and k_y is the strengthening coefficient.

Microstructure plays key roles not only in the mechanical properties but also the kinetic pathways of certain phase transformations. For instance, dislocations can act to catalyze precipication in binary alloys [cite Vahid].

The problem that we face is then, how do we examine these defects and microstructural elements but retain some of the successful aspects of density functional approach? One way

to think about to consider the microstructure in the solid state is that it is an artifact of not having fulling reached equilibrium. Real materials are solidified over a finite time and therefore haven't fully reached equilibrium. As a result, we should study the pathway to equilibrium to gain insight into the origin of microstructure.

3.2 Dynamic Density Functional Theory

Using techniques from non-equilibrium statistical mechanics we can extend the density functional approach to a dynamic model. To start we illustrate the non-equilibrium method schematically. Consider a non-equilibrium probability distribution over phase space, $f(\mathbf{q}, \mathbf{p}; t)$. As a function over phase space, its equation of motion is a simple result of classical mechanics,

$$\frac{df}{dt} = \{f, \mathcal{H}\} + \frac{\partial f}{\partial t}. \tag{3.9}$$

Where, $\{\cdot, \cdot\}$, denotes the Poisson bracket,

$$\{f, g\} = \sum_{i=0}^{N} \frac{\partial f}{\partial q_i}\frac{\partial g}{\partial p_i} - \frac{\partial g}{\partial q_i}\frac{\partial f}{\partial p_i}. \tag{3.10}$$

Of course, the distribution must remain normalized in time and therefore the total time derivative must be zero,

$$\int d\mathbf{q}d\mathbf{p}\, f(\mathbf{q}, \mathbf{p}; t) = 1 \rightarrow \frac{df}{dt} = 0. \tag{3.11}$$

Accounting for this conservation law in equation 3.9, the resulting equation of motion is called the *Liouville Equation*,

$$\frac{\partial f}{\partial t} = -\{f, \mathcal{H}\} \tag{3.12}$$

Under appropriate conditions the probability distribution, under the action of the Liouville Equation, will decay to a stable fixed point $f_{eq}(\mathbf{q}, \mathbf{p})$ we call equilibrium,

$$\lim_{t\to\infty} f(\mathbf{q}, \mathbf{p}; t) = f_{eq}(\mathbf{q}, \mathbf{p}) \tag{3.13}$$

Using the non-equilibrium probability distribution, we can also discuss non-equilibrium averages of the density profile and their associated equations of motions. The non-equilibrium density is written in analogy with equation 2.15 by taking of the classical trace of the density operator over with the non-equilibrium distribution,

$$\rho(x, t) = \langle \hat{\rho}(x; \mathbf{q}) \rangle_{ne} = \mathrm{Tr}\left[\hat{\rho}(x; \mathbf{q}) f(\mathbf{q}, \mathbf{p}, t)\right]. \tag{3.14}$$

Where, $\langle \cdot \rangle_{ne}$, denotes the non-equilibrium average. Just as the non-equilibrium probability distribution is driven to equilibrium by the Liouville Equation, so too is the density profile by its own equation of motion.

A variety of equations of motion for the density field are known. For instance, we can consider the Navier-Stokes equations of hydrodynamics to one such equation of motion. If we restrict ourselves to diffusion limited circumstances, we may derive a much simplier equation of motion. To acheive this result we use the projection operator method, and assume that the density operator is the only relevant variable. Quoting the result from [2] we find,

$$\frac{\partial \rho(x, t)}{\partial t} = \nabla \cdot \int \mathrm{d}r' \, \mathbf{D}(r, r', t) \cdot \nabla' \frac{\delta \mathcal{F}[\rho]}{\delta \rho(x', t)}, \tag{3.15}$$

Where, $\mathbf{D}(r, r', t)$, is the diffusion tensor,

$$\mathbf{D}(r, r', t) = \int_0^\infty \mathrm{d}\tau' \, \mathrm{Tr}\left[f(\mathbf{q}, \mathbf{p}, t) \hat{\mathbf{J}}(r, 0) \hat{\mathbf{J}}(r', \tau')\right], \tag{3.16}$$

in which $\mathbf{J}(r,t)$ is the density flux is,

$$\hat{\mathbf{J}}(r,t) \equiv \sum_{i}^{N} \frac{p_i}{m_i} \delta(q_i - r). \tag{3.17}$$

Should we use assume

If we restrict ourselves to the case where transport is diffusion limited and we assume that the dynamic pair correlation function is the same as the equilibrium pair correlation we can express the density equation of motion as,

$$\frac{\partial \rho(x,t)}{\partial t} = \nabla \cdot \left[D_0 \rho(x,t) \nabla \left(\frac{\delta \mathcal{F}[\rho]}{\delta \rho(x,t)} \right) \right]. \tag{3.18}$$

Where, D_0 is the diffusion constant. We can also express the dynamics of the density field in the form of a Langevin equation for the density operator,

$$\frac{\partial \hat{\rho}(x,t)}{\partial t} = \nabla \cdot \left[D_0 \hat{\rho}(x,t) \nabla \left(\frac{\delta \mathcal{F}[\hat{\rho}]}{\delta \hat{\rho}} \right) \right] + \xi(x,t). \tag{3.19}$$

Where, $\xi(x,t)$ is a Gaussian random driving force with zero mean and variance of,

$$\langle \xi(x,t) \xi(x',t') \rangle = -2\nabla \cdot \left[D_0 \rho(x,t) \nabla \delta(x - x') \delta(t - t') \right], \tag{3.20}$$

Due to a generalized Einstein relation[2] for the Langevin equation in equation 3.19.

Equation 3.18 and 3.19 were first derived by Marconi and Tarazona by considering an ensemble of interacting Brownian particles, but other derivations are possible including the projection operator method [cite Espanol]. Equations 3.18 and 3.19 fall under the heading of *Dynamic Density Functional Theory* (DDFT) or sometimes *Time dependent density functional theory* (TD-DFT) though we'll use the former throughout this text.

Unfortunately, if we were to use the approximate free energy functional established in equation 2.43 in the dynamic density functional theory of equation 3.18 or 3.19 we would face

[2]See Appendix A for details on generalized Einstein relations for nonlinear Langevin equations

a major impedement: the solid state solutions of the density functional theory approach yield sharply peaked solutions at the position of the atoms in the lattice. While this is realistic, they are a major challenge for numerical algorithms. The challenges are two fold: first, these sharp peaks require a fine mesh to be resolved resulting in large memory requirement to simulate domains of any non-trivial scale and second, lineary stability analysis of most algorithms slave the scale of the time step to the scale of the grid spacing so only small time steps can be taken on a fine mesh.

3.3 Phase Field Crystal Theory

The phase field crystal theory (PFC) presents a solution to the numerical difficulties faced by DDFT methods by approximating the free energy in such a say as to retain the basic features of the theory with a smoother solid state solution. Starting the approximate free energy functional of equation 2.43 we proceed as previously by scaling out a factor of the reference density and changing variables to a dimensionless density $n(r) = (\rho(r) - \rho_l)/\rho_l$,

$$\frac{\beta\mathcal{F}[n(r)]}{\rho_l} = \int dr \left\{(n(r)+1)\ln(n(r)+1) - (1-\beta\mu)n(r)\right\} - \frac{1}{2}n(r) * \rho_l C_0^{(2)}(r,r') * n(r'). \tag{3.21}$$

We then Taylor expand the logarithm about the reference density or equivalently $n(r) = 0$, to fourth order,

$$\frac{\beta\mathcal{F}[n(r)]}{\rho_l} = \int dr \left\{\frac{n(r)^2}{2} - \frac{n(r)^3}{6} + \frac{n(r)^4}{12}\right\} - \frac{1}{2}n(r) * \rho_l C_0^{(2)}(r,r') * n(r'). \tag{3.22}$$

Where the linear term has been dropped because it leaves the equations of motion invariant. Most phase field crystal theories also use a simplified equation of motion as well,

$$\frac{\partial n(r,t)}{\partial t} = M\nabla^2\left(\frac{\delta\mathcal{F}[n(r)]}{\delta n(r)}\right). \tag{3.23}$$

Chapter 4

Simplified Binary Phase Field Crystal Models

In this chapter we will walk through three simplified binary PFC models. The first is the original binary PFC model, which, while highly successful at modelling a few important phenomena is ultimately limited in scope. The second is the binary structural phase field crystal, or binary XPFC which was successful in modelling a broad spectrum of crystalline structures, but was limited in its ability of model liquid instablilities and a variety of phase diagrams. Finally, we'll see a new contribution to which we will call the regular phase field crystal model which is successful in modeling a broad spectrum of invariant binary reactions and crystalline structures.

All binary PFC models begin with a multicomponent variant of the approximate free energy functional established in Chapter 2,

$$\beta\mathcal{F}[\rho_A,\rho_B] = \sum_{i=A,B}\int \mathrm{d}r\,\rho_i(r)\ln\left(\frac{\rho_i(r)}{\rho_i^0}\right) - (1-\beta\mu_i^0)\Delta\rho_i(r) \\ -\frac{1}{2}\sum_{i,j=A,B}\Delta\rho_i(r) * C_{ij}^{(2)}(r,r') * \Delta\rho_j(r'). \tag{4.1}$$

It is convenient to change variables to a dimensionless total density, $n(r)$ and local concen-

tration, $c(r)$,

$$n(r) = \frac{\Delta\rho}{\rho_0} = \frac{\Delta\rho_A + \Delta\rho_B}{\rho_A^0 + \rho_B^0} \tag{4.2}$$

$$c(r) = \frac{\rho_B}{\rho} = \frac{\rho_B}{\rho_A + \rho_B}. \tag{4.3}$$

Scaling out a factor of the total reference density, ρ_0 we can break the free energy functional in these new variables into three parts,

$$\frac{\beta\mathcal{F}[n,c]}{\rho_0} = \frac{\beta\mathcal{F}_{id}[n]}{\rho_0} + \frac{\beta\mathcal{F}_{mix}[n,c]}{\rho_0} + \frac{\beta\mathcal{F}_{ex}[n,c]}{\rho_0}, \tag{4.4}$$

Where,

$$\frac{\beta\mathcal{F}_{id}[n]}{\rho_0} = \int \mathrm{d}r \, \left\{(n(r)+1)\ln(n(r)+1) - (1-\beta\mu^0)n(r)\right\} \tag{4.5}$$

$$\frac{\beta\mathcal{F}_{mix}[n,c]}{\rho_0} = \int \mathrm{d}r \, \left\{(n(r)+1)\left(c\ln\left(\frac{c}{c_0}\right) + (1-c)\ln\left(\frac{1-c}{1-c_0}\right)\right)\right\}, \tag{4.6}$$

And, if we assume the local concentration $c(r)$ varies over much longer length scales than the local density $n(r)$,

$$\begin{aligned}\frac{\beta\mathcal{F}_{ex}[n,c]}{\rho_0} = &-\frac{1}{2}n(r) * [C_{nn}(r,r') * n(r') + C_{nc}(r,r') * \Delta c(r')] \\ &-\frac{1}{2}\Delta c(r) * [C_{cn}(r,r') * n(r') + C_{cc}(r,r') * \Delta c(r')]\,.\end{aligned} \tag{4.7}$$

We have introduced μ_0 as the total chemical potential of the reference mixture, $c_0 = \rho_B^0/\rho_0$ as the reference concentration and $\Delta c(r) = c(r) - c_0$ as the deviation of the concentration

from the reference. The $n-c$ pair correlation introduced in the excess free energy are,

$$C_{nn} = \rho_0 \left(c^2 C_{BB} + (1-c)^2 C_{AA} + 2c(1-c) C_{AB} \right) \tag{4.8}$$

$$C_{nc} = \rho_0 \left(c C_{BB} - (1-c) C_{AA} + (1-2c) C_{AB} \right) \tag{4.9}$$

$$C_{cn} = C_{nc} \tag{4.10}$$

$$C_{cc} = \rho_0 \left(C_{BB} + C_{AA} - 2C_{AB} \right) \tag{4.11}$$

Explicit calculations can be found in Appendix C. Differences in the various simplified binary PFC theories stem from differing approximations of the terms in the free energy stated in equation 4.4.

4.1 Original Binary Phase Field Crystal Model

In the original simplified binary PFC theory, all terms in the free energy are expanded about $n(r) = 0$ and $c(r) = c_0$ (ie., about their reference states). For the ideal free energy this results in a polynomial truncated to fourth order,

$$\frac{\beta \mathcal{F}_{id}[n]}{\rho_0} = \int \mathrm{d}r \left\{ \frac{n(r)^2}{2} - \frac{n(r)^3}{6} + \frac{n(r)^4}{12} \right\}. \tag{4.12}$$

The linear term is dropped due to invariance in the equations of motion. If we assume for simplicity of demonstration $c_0 = 1/2$, the free energy of mixing becomes a simple fourth order polynomial as well,

$$\frac{\beta \mathcal{F}_{mix}[n,c]}{\rho_0} = \int \mathrm{d}r \left\{ 2\Delta c(r)^2 + \frac{4\Delta c(r)^4}{3} \right\}. \tag{4.13}$$

Linear couplings to $n(r)$ are dropped by assuming, as we already have, that the concentration field varies on a much longer length scale than the total density and noting that the total density is defined about its average. This argument can also be applied the linear couplings

to $n(r)$ in the excess free energy term which leaves only the C_{nn} and C_{cc} terms. Finally, these two terms are approximated with a gradient expansions of the correlation functions,

$$C_{nn}(r,r') = \delta(r-r')\left(\alpha + \beta\nabla^2 + \gamma\nabla^4 + \ldots\right), \tag{4.14}$$

$$C_{cc}(r,r') = \delta(r-r')\left(\epsilon + \xi\nabla^2 + \ldots\right). \tag{4.15}$$

The expansion parameters, α, β, and γ are all dependent on temperature and concentration. We are required to expand C_{nn} to fourth order because, as noted in chapter 3 the peak of the direct correlation function in Fourier space is the driving force for solidification. The concentration field is correlated over a longer length scale implying that only the short wavevectors are important in C_{cc} so we can expand just to quadratic order.

Gathering terms the resulting free energy functional for the original simplified binary PFC model[1] is,

$$\begin{aligned}\frac{\beta\mathcal{F}[n,c]}{\rho_0} = &\int \mathrm{d}r\, \left\{\frac{1}{2}n(r)\left(1-\alpha-\beta\nabla^2-\eta\nabla^4\right)n(r) - \frac{n(r)^3}{6} + \frac{n(r)^4}{12}\right\} \\ &+ \int \mathrm{d}r\, \left\{\frac{1}{2}\Delta c(r)\left(4-\epsilon-\xi\nabla^2\right)\Delta c(r) + \frac{4\Delta c(r)^4}{3}\right\}.\end{aligned} \tag{4.16}$$

The strength of the original simplified binary PFC model is that is retains most of the important physics of binary alloys in a very reduced theory. For instance, the simplified model is capable of describing the equilibrium phase diagrams of both eutectic alloys alloys and materials with a solid state spinodal / liquid minimum. Supplied with a diffusive equation of motion the simplified model can model an impressive diversity of dynamic phenomena including eutectic growth, phase segregation, dendritic growth, dislocation motion in solid state spinodal coarsening and epitaxial growth.

The major limitation of the original simplified model is that the gradient expansion of the density-density correlation function gives only a crude control over the structures that

[1]The orignal simplified binary PFC model was expressed using slightly different variables. We expand in $\Delta c(r)$ here to facilitate comparison with other theories

will be formed. In fact, as this theory only controls a single peak in Fourier space it can only solidify into the fcc phase [check this is the case for the original theory]. As noted in chapter 3. The ability to solidify into an arbitrary structure demands control of value of the density-density correlation function at all reciprocal lattice vectors.

A second limitation of the original simplified model is that it is local in concentration. This means that realistic phase diagrams from 0 to 100% concentration cannot be produced, only local phase diagrams around the reference concentration that was expanded about. To construct these global phase diagrams we require the entire free energy of mixing term in equation 4.6.

4.2 Binary Structural Phase Field Crystal Model

The binary structural phase field crystal theory (XPFC) seeks to remedy the two short comings of the original simplified model. That is, it seeks to construct realistic phase diagrams for binary systems and seeks to reproduce a variety of crystal lattice structure. We'll begin with a derivation of the theory and compare with the original model.

First, the ideal free energy is expanded in precisely the same manner resulting in the same fourth order polynomial,

$$\frac{\beta\Delta\mathcal{F}_{id}[n]}{\rho_0} = \int \mathrm{d}r \left\{ \frac{n(r)^2}{2} - \eta\frac{n(r)^3}{6} + \chi\frac{n(r)^4}{12} \right\}. \qquad \text{(4.12 revisited)}$$

The free energy of mixing is left unexpanded but an overall scale ω is added to fit the mixing term away from the reference concentration,

$$\frac{\beta\mathcal{F}_{mix}[n,c]}{\rho_0} = \int \mathrm{d}r \left\{ \omega(n(r)+1)\left(c\ln\left(\frac{c}{c_0}\right) + (1-c)\ln\left(\frac{1-c}{1-c_0}\right)\right)\right\}. \qquad (4.17)$$

This unexpanded free energy of mixing will lead to more accurate global phase diagrams. The excess free energy is approximated using the similar assumptions as in the original model

(linear couplings are dropped), but the density-density correlation function is not expanded. Greenwood *et al* all assumed that the $k = 0$ mode of the concentration-concentration correlation function was zero leaving only the quadratic term in the expansion,

$$C_{cc}(r, r') = \delta(r - r')\alpha\nabla^2. \tag{4.18}$$

Grouping terms together, the complete free energy functional for the binary XPFC model is,

$$\begin{aligned}\frac{\beta\Delta\mathcal{F}[n, c]}{\rho_0} = &\int \mathrm{d}r \left\{\frac{1}{2}n(r)\left(1 - C_{nn}(r, r')\right) * n(r') - \eta\frac{n^3}{6} + \chi\frac{n^4}{12}\right\} \\ &+ \int \mathrm{d}r \left\{\frac{1}{2}\left|\nabla c(r)\right|^2 + \omega f_{mix}(r)\right\}.\end{aligned} \tag{4.19}$$

Where $f_{mix}(r)$ is the local free energy density of mixing,

$$f_{mix}(r) = (n(r) + 1)\left(c(r)\ln\left(\frac{c(r)}{c_0}\right) + (1 - c(r))\ln\left(\frac{1 - c(r)}{1 - c_0}\right)\right). \tag{4.20}$$

4.2.1 Modelling Correlation Functions

The key insight made by the XPFC model the that, the density-density correlation function can be modelled in such a way as to control the crystall lattice structure targetted under cooling and to target different structures at different concentrations. Note that the density-density correlation function as the form of a linear combination of interpolating functions in concentration, $\zeta(c)$, multiplied by bare correlation functions $C(r, r')$,

$$C_{nn}(r, r'; c) = \sum_i \zeta_i(c)C_i(r, r') \tag{4.21}$$

In the exact theory, for example, we have,

$$\zeta_{AA}(c) = \rho_0(1 - c^2), \tag{4.22}$$

$$\zeta_{AB}(c) = \rho_0 c(1 - c), \tag{4.23}$$

$$\zeta_{BB}(c) = \rho_0 c^2. \tag{4.24}$$

Each interpolating function, $\zeta_i(c)$, defines a domain of validity for its associated correlation function $C_i(r, r')$. This suggests that we might model any density-density correlation function using this general structure: the set of correlation function $C_i(r, r')$ enumerate the various structures that may manifest themselves and the associated interpolation functions $\zeta_i(c)$ define the concentrations over which these correlations are valid.

As a simple example we wanted to construct a simple model of the silver-cupper eutectic alloy system, we might start with some model correlation function for pure silver, $C_\alpha(r, r')$, and for pure copper, $C_\beta(r, r')$. These two structures, the silver rich α phase and the copper rich β phase, are the only two relevent crystalline structures in the system so to build the full density-density correlation function we just need to choose interpolating functions for each. Following Greenwood *et al* for example, we might choose,

$$\zeta_\alpha(c) = 1 - 3c^2 + 2c^3, \tag{4.25}$$

$$\zeta_\beta(c) = 1 - 3(1 - c)^2 + 2(1 - c)^3. \tag{4.26}$$

This leaves the question of how to develop model correlation functions for any particular crystalline lattice of interest. This problem is also anwsered by the XPFC framework. Originally delineated for pure systems, the XPFC method for constructing correlation functions is strongly influenced by the methods developed by Ramakrishnan. In particular this means that, given that the driving force for solidification is the of value direct correlation function at the reciprocal lattice vectors, we need a model correlation function that controls these

parameters specifically. We can acheive this with Gaussian peaks centred at the reciprocal lattice vector positions,

$$C_i(r, r') = \sum_{\alpha} e^{\frac{T}{T_i^0}} e^{-\frac{(k-k_i)^2}{2\sigma_i^2}} \tag{4.27}$$

Where, as in chapter 3, the index α runs over families of point group equivalent reciprocal lattice vectors. The temperature dependent prefactors e^{T/T_i^0} give the correct temperature scaling of the amplitudes close to the melting point[2] as discussed by [1].

The advantages of the XPFC simplified binary model are two fold: realistic phase diagrams and modelling a variety of crystalline lattices. While the former is relatively cosmetic the latter allows for the examination of guininely novel systems in comparison with the original simplified model. For example the binary XPFC model as been used to study, peritectic systems, ordered crystals, [find refs and list of applications] [5, 1].

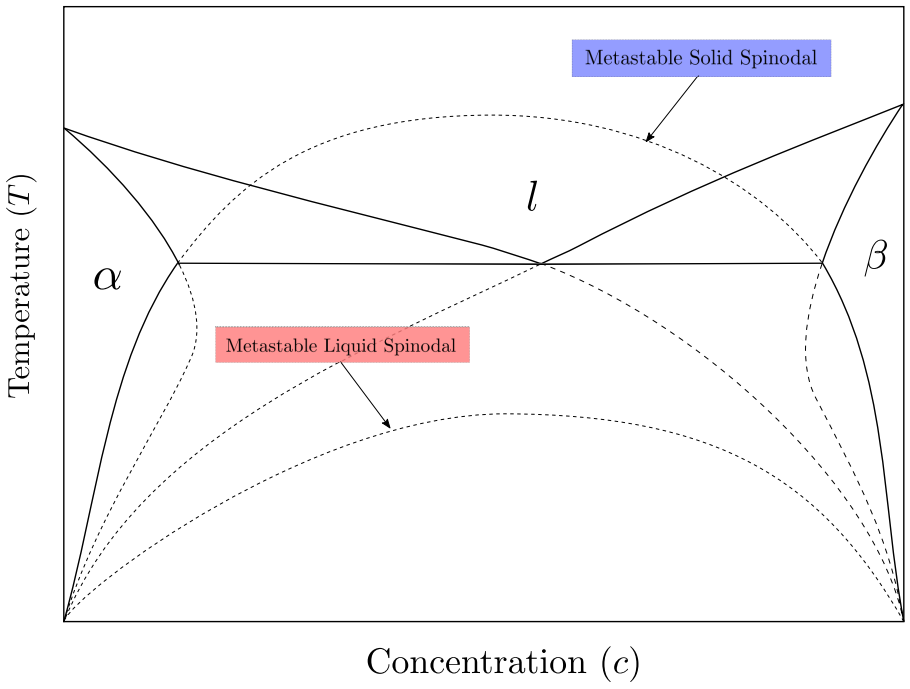

Figure 4.1: Eutectic phase diagram with metastable projects. Stable coexistance lines are rendered solid where as metastable projections are dashed.

Unfortunately, by assuming that the $k = 0$ mode of the concentration-concentration

[2]The original XPFC works used a phenomonological prefacter with e^{T^2/C_i} for a constant C_i. This choice is inspired by harmonic analysis in the solid phase and the Debye-Waller factor

correlation function is zero the XPFC model restricts the its free energy of mixing to an ideal model of mixing. This model of mixing includes only entropic contributions to the free energy. This means that the sole driving force for phase seperation is elastic energy as the heat of mixing is always positive (right? I always mess up this convention). This can be a limitation on modelling a variety of binary alloy systems, for instance both monotectic and syntectic systems cannot be modelled without a negative heat of mixing. More subtly, even eutectic systems have a negative heat of mixing deep below the eutectic point as the metastable liquid has a spinodal. This phenomena is shown shown schematically in figure 4.1 where the metastable projections, including solid and liquid spinodals, are drawn on a hypothetical eutectic phase diagram. Problems such as the stability of nanocrystalline binary alloys require an examination of the balance of elastic energies and bulk mixing free energy [15].

4.3 Regular Phase Field Crystal Model

The regular phase field crystal model is a simplified model that aims to combine the positive aspects of the XPFC and original simplified models together. The original PFC model uses an regular model of mixing so both enthalpic and entropic contribution to the free energy of mixing are considered. This is acheived by assuming there is a $k = 0$ contribution in the gradient expansion of the concentration-concentration correlation function. If we add this simple component to the development of the XPFC free energy functional we find one additional term that gives an enthaly of mixing,

$$\begin{aligned}\frac{\beta\Delta\mathcal{F}[n,c]}{\rho_0} = &\int \mathrm{d}r \left\{\frac{1}{2}n(r)\left(1 - C_{nn}(r,r')\right) * n(r') - \eta\frac{n^3}{6} + \chi\frac{n^4}{12}\right\} \\ &+ \int \mathrm{d}r \left\{\frac{1}{2}\left|\nabla c(r)\right|^2 + \omega f_{mix}(r)\right\}.\end{aligned} \tag{4.28}$$

Where the local free energy density of mixing, f_{mix} is now,

$$f_{mix}(r) = (n(r)+1)\left(c(r)\ln\left(\frac{c(r)}{c_0}\right) + (1-c(r))\ln\left(\frac{1-c(r)}{1-c_0}\right)\right) + \frac{1}{2}\epsilon(c-c_0)^2. \quad (4.29)$$

The simplicity the temperature dependence if the parameter ϵ is taken to be linear about the spinodal temperature T_c,

$$\epsilon(T) = -4 + \epsilon_0(T - T_c). \quad (4.30)$$

4.3.1 Equilibrium Properties

Here we'll explore the flexibility of the simplified regular PFC model in describing various material phase diagrams in binary systems.

Eutectic Phase Diagram

While previous PFC models have shown that elastic energy is a sufficient driving force for eutectic solidification our simplified regular model allows for the examination of the role enthalpy of mixing can play in eutectic solids. For instance, Murdoch and Schuh noted that in nanocrystalline binary alloys, while a positive enthaply of segregation can stabilize against grain growth via solute segregation at the grain boundary, if the enthaply of mixing becomes too large this effect can be negated by second phase formation or even macroscopic phase seperation[15].

To specialize our simplified regular model to the case of the binary eutectic we must choose an appropriate model for the correlation function. Choosing an α phase around $c = 0$ and β phase around $c = 1$, we can recover the pair correlation function used in the binary

XPFC with a particular choice of window functions:

$$\zeta_\alpha(c) = 2c^3 - 3c^2 + 1 \tag{4.31}$$

$$\zeta_\beta(c) = \zeta_\alpha(1-c). \tag{4.32}$$

Should we choose, for example, an α and β phase with 2 dimensional hexagonal lattices, differing only by lattice constants, we can produce a phase diagram like that in Fig. 4.2.

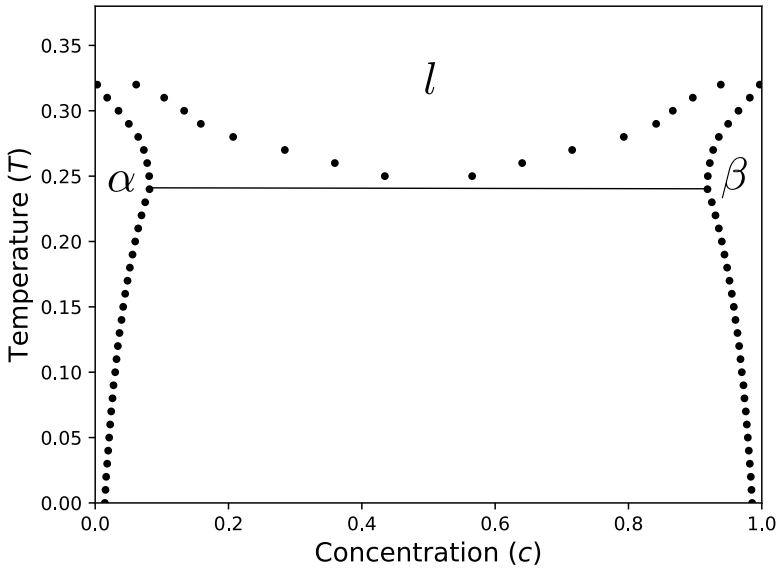

Figure 4.2: Eutectic phase diagram triangle α and β phases. The free energy parameter are $\eta = 2$, $\chi = 1$, $\omega = 0.30$, $\epsilon_0 = 3$ and $T_c = 0.01$. The parameters of the structure functions are $\alpha_{10\alpha} = \alpha_{10\beta} = 0.8$, $k_{10\alpha} = 2\pi$, $k_{10\beta} = 4\pi/\sqrt{3}$ and $T_0 = 1$

Syntectic Phase Diagram

Our regular model also allows for the study of a variety of invariant binary reactions that, to date, have not been studied using phase field crystal models. One such reaction is the syntectic reaction.

The syntectic reaction, $l_1 + l_2 \rightarrow \alpha$, consists of solidification at the interface of two liquids. We can achieve this with our model by setting the spinodal temperature, T_c, sufficiently high

and producing a density-density correlation function that is peaked at a concentration below the spinodal. This can be done by choosing a window function that is centered about an intermediate concentration, c_α of the solid phase, α.

$$\chi(c) = e^{-\frac{(c-c_\alpha)^2}{2\alpha_c}} \tag{4.33}$$

The resulting correlation function for a hexagonal lattice in two dimensions, for example, would be,

$$\tilde{C}_{nn}(k;c) = e^{-\frac{(c-c_\alpha)^2}{2\alpha_c}} e^{-\frac{T}{T_0}} e^{-\frac{(k-k')^2}{2\alpha^2}} \tag{4.34}$$

A phase diagram that produces a syntectic reaction with an appropriate choice of parameters can be seen in Fig. 4.3.

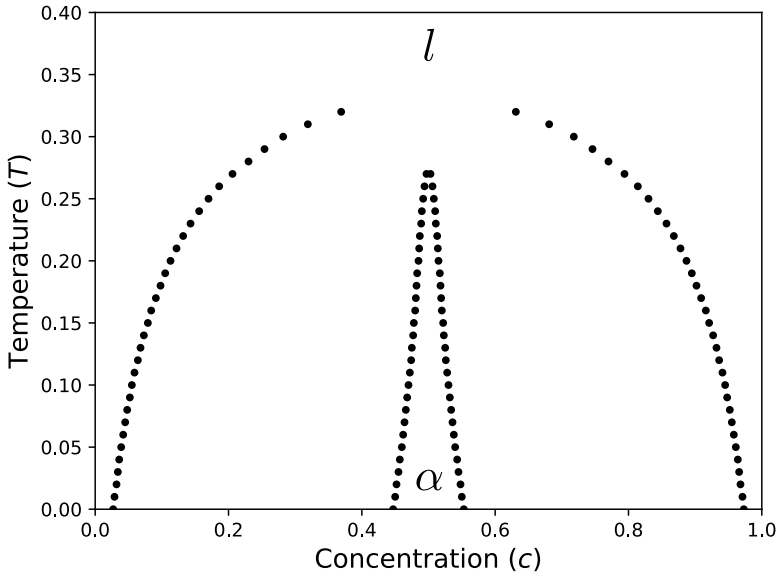

Figure 4.3: Phase Diagram of Syntectic Alloy with a hexagonal α phase. The free energy parameters are $\eta = 2$, $\chi = 1$, $\omega = 0.3$, $\epsilon_0 = 10$ and $T_c = 0.35$. The parameters for the structure function are $\alpha_{10\alpha} = 0.8$, $k_{10\alpha} = 2\pi$ and $T_0 = 1$

Monotectic Phase Diagram

The monotectic reaction is another invariant binary reaction that has not previously been studied using PFC models. The monotectic reaction, $l_1 \rightarrow \alpha + l_2$, consists of decomposing liquid into a solute poor solid and solute rich liquid. To model a monotectic using our regular model we hypothesize a solid phase at $c = 0$ and set the spinondal temperature higher than the solidification temperature. To achieve this we use a window function peaked around $c = 0$,

$$\chi_\alpha(c) = e^{-\frac{c^2}{2\alpha_c^2}}. \tag{4.35}$$

Again considering a simple hexagonal lattice for the α phase, we can produce a phase diagram with a monotectic reaction with an appropriate choice of parameters as in Fig. 4.4.

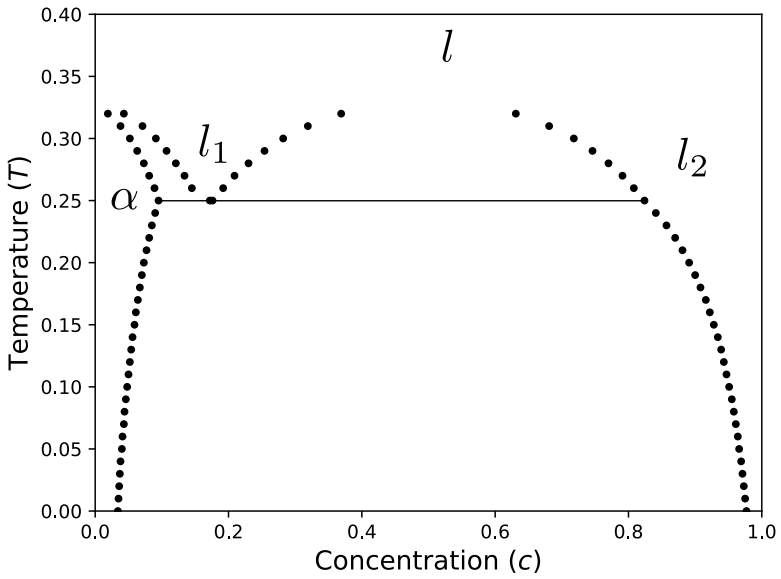

Figure 4.4: Phase Diagram of Monotectic Alloy with hexagonal α phase. The free energy parameters are $\eta = 2$, $\chi = 1$, $\omega = 0.3$, $\epsilon_0 = 10$, $T_c = 0.35$ and $c_0 = 0.75$. The parameters for the structure function are $\alpha_{10\alpha} = 0.8$, $k_{10\alpha} = 2\pi$ and $T_0 = 1$ and the parameter for the window function is $\alpha_c = 0.4$

Precipitation from Solution

We can also model precipitation of nanoparticles from solution. While on its surface the equilibrium phase diagram of a solution is that of a simple solid-liquid coexistance, in practice the metastable features of the phase diagram can have profound implications on the nucleation kinetics of precipitate. As an example, precipitation from solution is a typical synthesis technique for gold and silver nanoparticles. Recent work by Loh *et al* shows that a metastable spinodal may be playing an important role in the growth and nucleation of gold nanoparticles under certain diffusive circumstances.

Using the regular XPFC model we can reproduce the condition of a metastable liquid spinodal underneath the liquid-solid coexistance curve. The approach to produce a phase diagram is the same as that of of a monotectic, with the exception that the spinodal temperature, T_c, most now be sufficiently low to be buried underneath the coexistance curve. In keeping with the concentration being that of the solute, we'll also center the gaussian window function about $c = 1$. An example, including metastable spinodal, can be seen in Fig. 4.5.

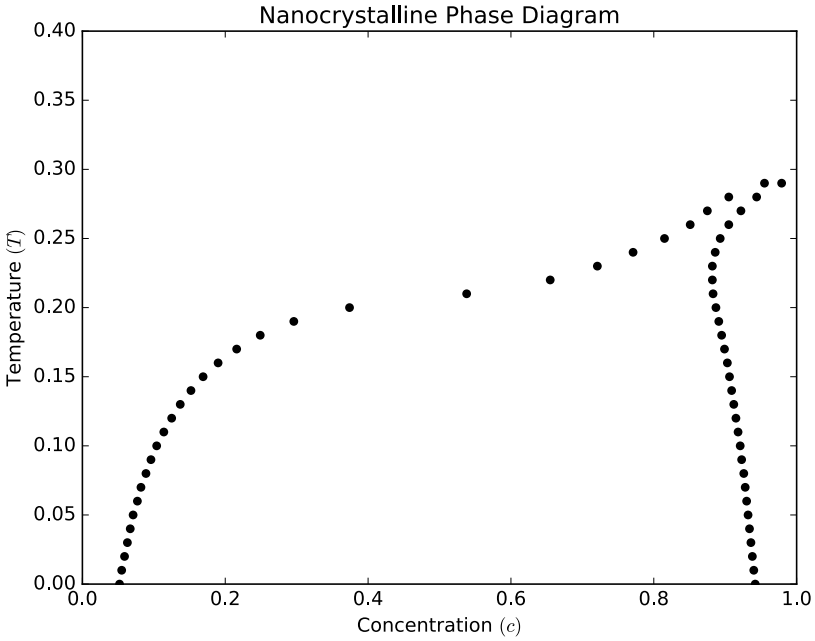

Figure 4.5: Phase Diagram of Solution fill me in please!!

Conclude the chapter with discussion of where what we've seen and lead into the discussion for the next chapter of dynamics and applications of this theory to more than just simple equilibrium phase diagrams

Chapter 5

Applications

In this chapter we discuss applications of our improvements to the binary XPFC model. To begin we'll discuss an effective equation of motion in the limit that density change on solidification is small, after which we'll examine the to process of multi-step nucleation of nanoparticles from solution. To conclude we'll discuss areas of future application.

5.0.1 Dynamics in the small Δn limit

Develop the dynamics from DDFT and show (with references to the relevant papers that these dynamics are valid in the small density change limit specifically

5.1 Multistep Nucleation of Nanoparticles in Solution

Discuss the interest in this process with reference to papers about multistep nucleation theories. Discuss relevance of nanoparticles size and prediction of size (catalyzsis, color, etc... size is the basic relevant detail of nanoparticles).

5.2 Future Applications

Appendix A

Noise in Nonlinear Langevin Equations

When using Langevin equations to study non-equilibrium statistical mechanics, the noise strength can be linked to the transport coefficients through a generalization of the Einstein relation. The generalization was first developed by Onsager and Machlup [16]. The typical strategy for deriving such a relationship is to evaluate the equilibrium pair correlation function by two separate methods: the equilibrium partition functional and the equation of motion[1].

While the equilibrium partition functional gives pair correlation through the typical statistical mechanical calculation, the equation of motion can be used to derive a dynamic pair correlation function that must be equal to the equilibrium pair correlation function in the long time limit.

In what follows we'll look at how to formulate a generalized Einstein relation from a generic Langevin equation and then calculate two specific examples using Model A dynamics and a ϕ^4 theory and Time Dependent Density Functional Theory (TDDFT) and a general Helmholtz free energy.

[1]For considerations far from equilibrium see [13, 18, 3]

A.1 Generalized Einstein Relations in an Arbitrary Model

We start by considering a set of microscopic observables, $a_i(r,t)$, that are governed by a nonlinear Langevin equation,

$$\frac{\partial \mathbf{a}(r,t)}{\partial t} = F[\mathbf{a}(r,t)] + \boldsymbol{\xi}(r,t). \tag{A.1}$$

Where, $\mathbf{a}$, denotes a vector of our fields of interest. These microscopic equation of motion may have been derived from linear response, projection operators or some other non-equilibrium formalism. We assume that the random driving force, $\boldsymbol{\xi}(r,t)$ is unbaised, Gaussian noise that is uncorrelated in time.

$$\langle \boldsymbol{\xi}(r,t) \rangle = 0 \tag{A.2}$$

$$\left\langle \boldsymbol{\xi}(r,t)\boldsymbol{\xi}^{\dagger}(r',t') \right\rangle = \mathbf{L}(r,r')\delta(t-t') \tag{A.3}$$

We wish to constrain the form of the covariance matrix, $\mathbf{L}$, by demanding that the solution to the Langevin equation eventually decays to equilibrium and that correlations in equilibrium are given by Boltzmann statistics.

We begin by linearizing the equation of motion about an equilibrium solution, $\mathbf{a}(r,t) = \mathbf{a}_{eq}(r) + \hat{\mathbf{a}}(r,t)$.

$$\frac{\partial \hat{\mathbf{a}}(r,t)}{\partial t} = \mathbf{M}(r,r') * \hat{\mathbf{a}}(r',t) + \boldsymbol{\xi}(r,t) \tag{A.4}$$

Where, $*$ denotes an inner product and integration over the repeated variable. eg:

$$\mathbf{M}(r,r') * \hat{\mathbf{a}}(r') = \sum_j \int dr' M_{ij}(r,r')\hat{a}_j(r'). \tag{A.5}$$

We can formally solve our linearized equation of motion,

$$\hat{\mathbf{a}}(r,t) = e^{\mathbf{M}(r,r')t} * \hat{\mathbf{a}}(r',0) + \int_0^t d\tau\, e^{\mathbf{M}(r,r')(t-\tau)} * \boldsymbol{\xi}(r',\tau), \tag{A.6}$$

And use this formal solution to evaluate the dynamic pair correlation function.

$$\begin{aligned}\left\langle \hat{\mathbf{a}}(r,t)\hat{\mathbf{a}}^{\dagger}(r',t')\right\rangle &= e^{\mathbf{M}(r,r_1)t} * \left\langle \hat{\mathbf{a}}(r_1,0)\hat{\mathbf{a}}^{\dagger}(r_2,0)\right\rangle * e^{\mathbf{M}^{\dagger}(r',r_2)t'} \\ &+ \int_0^t \int_0^{t'} d\tau d\tau' \, e^{\mathbf{M}(r,r_1)(t-\tau)} * \left\langle \boldsymbol{\xi}(r_1,0)\boldsymbol{\xi}^{\dagger}(r_2,0)\right\rangle * e^{\mathbf{M}^{\dagger}(r',r_2)(t'-\tau')} \end{aligned} \tag{A.7}$$

To evaluate the equilibrium correlation function we take the limit as each time goes to infinity together ($t = t' \to \infty$). It is important to note that every eigenvalue of $\mathbf{M}$ must be negative for our solution to decay to equilibrium in the long time limit (eg. $lim_{t\to\infty}\hat{\mathbf{a}}(r,t) = 0$) and as such the first term in our dynamic correlation function won't contribute to the equilibrium pair correlation. This is as we might expect as the first term holds the contributions to the dynamic correlation function from the initial conditions. The second term can be evalutated by substituting the noise correlation and evaluating the delta function.

$$\boldsymbol{\Gamma}(r,r') = \lim_{t\to\infty} \left\langle \hat{\mathbf{a}}(r,t)\hat{\mathbf{a}}^{\dagger}(r',t)\right\rangle = \int_0^{\infty} dz \, e^{\mathbf{M}(r,r_1)z} * \mathbf{L}(r_1,r_2) * e^{\mathbf{M}^{\dagger}(r',r_2)z} \tag{A.8}$$

Considering the product $\mathbf{M}(r,r_1) * \boldsymbol{\Gamma}(r_1,r')$ and performing an integration by parts gives the final generalized Einstein relation.

$$\mathbf{M}(r,r_1) * \boldsymbol{\Gamma}(r_1,r') + \boldsymbol{\Gamma}(r,r_1) * \mathbf{M}^{\dagger}(r_1,r') = -\mathbf{L}(r,r') \tag{A.9}$$

A.2 Example 1 - Model A

As a first example of calculating an Einstein relation consider the following free energy functional under non-conservative, dissipative dynamics.

$$\beta\mathcal{F}[\phi] = \int dr \left\{ \frac{1}{2}|\nabla\phi(x)|^2 + \frac{r}{2}\phi^2(x) + \frac{u}{4!}\phi^4(x) + h(x)\phi(x) \right\} \tag{A.10}$$

$$\frac{\partial\phi(x,t)}{\partial t} = -\Gamma\left(\frac{\delta\beta\mathcal{F}[\phi]}{\delta\phi(x)}\right) + \xi(x,t) \tag{A.11}$$

The random driving force, ξ, is Gaussian noise, uncorrelated in time.

$$\langle \xi(x,t) \rangle = 0 \tag{A.12}$$

$$\langle \xi(x,t)\xi(x',t') \rangle = L(x-x')\delta(t-t') \tag{A.13}$$

To compute the Einstein relation for this theory we start by calculating the pair correlation function using the equilibrium partition function and Boltzmann statistics.

A.2.1 The partition function route

In equilibrium the probability of particular field configuration is given by the Boltzmann distribution.

$$\mathcal{P}_{eq}[\phi] = \frac{e^{-\beta \mathcal{F}[\phi]}}{\mathcal{Z}[h(x)]} \tag{A.14}$$

Where, $\mathcal{Z}[h(x)]$ is the partition functional and is given by a path integral over all field configurations.

$$\mathcal{Z}[h(x)] = \int \mathcal{D}[\phi] e^{-\beta \mathcal{F}[\phi]} \tag{A.15}$$

Evaluation of the partition function is of some importance because it plays the role of a moment generating function.

$$\frac{1}{\mathcal{Z}[h]} \frac{\delta^n \mathcal{Z}[h]}{\delta h(x_1) ... \delta h(x_n)} = \langle \phi(x_1) ... \phi(x_n) \rangle \tag{A.16}$$

In general the partition function cannot be computed directly, but in the special case of Gaussian free energies it can. To that end we consider expanding ϕ around an equilibrium solution, $\phi(x) = \phi_0 + \Delta\phi(x)$, and keeping terms to quadratic order in the free energy.

$$\beta \mathcal{F}[\Delta\phi] = \int dr \left\{ \frac{1}{2} \Delta\phi(x) \left(r - \nabla^2 + \frac{u}{2}\phi_0^2 \right) \Delta\phi(x) - h(x)\Delta\phi(x) \right\} \tag{A.17}$$

Here the partition function is written in a suggestive form. As stated previously, functional integrals are difficult to compute in general, but Gaussian functional integrals do have a solution.

Computing the Pair correlation function in the Gaussian approximation

To compute the pair correlation function we use the Fourier space variant of the partition function,

$$\mathcal{Z}[\tilde{h}(k)] \propto \exp\left\{\frac{1}{2}\int dk\, \frac{h(k)h^*(k)}{r+\frac{u}{2}\phi_0^2+|k|^2}\right\}. \tag{A.18}$$

The pair correlation function, $\langle\Delta\tilde{\phi}(k)\Delta\tilde{\phi}^*(k)\rangle$, is then computed using equation A.16.

$$\left\langle\Delta\tilde{\phi}(k)\Delta\tilde{\phi}^*(k')\right\rangle = \frac{2\pi\delta(k+k')}{r+\frac{u}{2}\phi_0^2+|k|^2} \tag{A.19}$$

A.2.2 The Equation of Motion Route

The equation of motion supplies a second method for evaluating the pair correlation function in equilibrium.

$$\frac{\partial\phi}{\partial t} = -\Gamma\left((r-\nabla^2)\phi(x,t)+\frac{u}{3!}\phi^3(x,t)\right)+\xi(x,t), \tag{A.20}$$

Our equation of motion, can be linearized around an equilibrium solution, ϕ_0, just as we did in the partition function route to the pair correlation function. In a similar vain, we will Fourier transform the equation of motion as well.

$$\frac{\partial\Delta\tilde{\phi}(k,t)}{\partial t} = -\Gamma\left((r+\frac{u}{2}\phi_0+|k|^2)\Delta\tilde{\phi}(k,t)\right)+\xi(x,t) \tag{A.21}$$

Comparing with our generalized approach we can read of $M(k,k')$ from the lineared equation of motion:

$$M(k,k') = -\Gamma\left((r+\frac{u}{2}\phi_0+|k|^2)\right)\delta(k+k') \tag{A.22}$$

Finally, once we compute the generalized Einstein relation with our specific pair correlation and $M(k,k')$ we find,

$$L(k,k') = 2\Gamma\delta(k+k'), \tag{A.23}$$

Or equivalently,

$$L(x,x') = 2\Gamma\delta(x-x'). \tag{A.24}$$

A.3 Example 2 - Time Dependent Density Functional Theory

In time dependent density functional theory (TDDFT) we have an equation of motion of the following form,

$$\frac{\partial\rho(r,t)}{\partial t} = D_0\nabla\cdot\left[\rho(r,t)\nabla\left(\frac{\delta\mathcal{F}[\rho]}{\delta\rho}\right)\right] + \xi(r,t) \tag{A.25}$$

Where, D_0 is the equilibrium diffusion constant and ξ is the stochastic driving force. We assume once again that the driving force has no bias, but we now allow the noise strength to be a generic kernel $L(r,r')$.

$$\langle\xi(r,t)\rangle = 0 \tag{A.26}$$

$$\langle\xi(r,t)\xi(r',t')\rangle = L(r,r')\delta(t-t') \tag{A.27}$$

A.3.1 Pair Correlation from the Partition Functional

Just like with the phi^4 model we want to expand our free energy functional around an equilibrium solution. In this case our free energy functional is generic so this expansion is

purely formal.

$$\mathcal{F}[\rho] = \mathcal{F}_{eq} + \beta \int dr \left(\frac{\delta \mathcal{F}[\rho]}{\delta \rho(r)} \right) \Bigg|_{\rho_{eq}} \Delta\rho(r) + \frac{1}{2} \int dr \int dr' \Delta\rho(r) \left(\frac{\delta^2 \mathcal{F}[\rho]}{\delta\rho(r)\delta\rho(r')} \right) \Bigg|_{\rho_{eq}} \Delta\rho(r') \tag{A.28}$$

The first term we can neglect as it adds an overall scale to the partition function that will not affect any of moments. Second moment only shifts the average so we can ignore it as well and so we're left with a simple quadratic free energy once again.

$$\mathcal{F}[\rho] = \frac{1}{2} \int dr \int dr' \Delta\rho(r) \Gamma^{-1}(r, r') \Delta\rho(r') \tag{A.29}$$

Where, $\Gamma^{-1}(r, r')$ is the second functional derivative of the free energy functional in equilibrium. Computing the pair correlation function from the partition function yields, as might be expected,

$$\langle \Delta\rho(r) \Delta\rho(r') \rangle = \Gamma(r, r') \tag{A.30}$$

A.3.2 Linearing the equation of motion

Linearizing the equation of motion about an equilibrium solution we find the following form,

$$\frac{\partial \Delta\rho(r,t)}{\partial t} = D_0 \nabla \cdot \left[\rho_{eq}(r) \nabla \left(\Gamma^{-1}(r, r') * \Delta\rho(r', t) \right) \right] + \xi(r, t) \tag{A.31}$$

Once again we can read of the kernel $M(r, r')$ from the linearized equation.

$$M(r, r\prime) = D_0 \nabla \cdot \left[\rho_{eq}(r) \nabla \left(\Gamma^{-1}(r, r') \right) \right] \tag{A.32}$$

Plugging into the generalized Einstein relation, we find a the factors of the pair correlation cancel giving a simple form for the kernel $L(r, r')$.

$$L(r, r') = -2D_0 \nabla \cdot \left(\rho_{eq}(r) \nabla \right) \delta(r - r') \tag{A.33}$$

Appendix B

Gaussian Functional Integrals

Gaussian Functional Integrals

In the study of the statistical physics of fields we often encounter functional integrals of the form,

$$\mathcal{Z}[h(x)] = \int \mathcal{D}[\phi] \exp\left\{ - \int dx \int dx' \left[\frac{1}{2} \phi(x) \mathbf{K}(x, x') \phi(x') \right] + \int dx \left[h(x) \phi(x) \right] \right\}. \quad \text{(B.1)}$$

Solutions to this integral are not only important in there own right but are also the basis perturbative techniques. The detail of how to solve this integral can be found in [9] and are repeated here for the convenience of the reader.

This integral is simply the continuum limit of a multivariable Gaussian integral,

$$\mathcal{Z}[\mathbf{h}] = \int \prod_i dx_i \exp\left\{ -\frac{1}{2} \sum_i \sum_j x_i \, \mathbf{K}_{ij} \, x_j + \sum_i h_i x_i \right\}, \quad \text{(B.2)}$$

For which the solution is,

$$\mathcal{Z}[\mathbf{h}] = \sqrt{\frac{2\pi}{\det(\mathbf{K})}} \exp\left\{ \frac{1}{2} \sum_i \sum_j h_i \mathbf{K}^{-1}_{ij} h_j \right\}. \quad \text{(B.3)}$$

In the continuum limit, the solution has an analogous form.

$$\mathcal{Z}[h(x)] \propto \exp\left\{\int dx \int dx' \left[\frac{1}{2}h(x)\mathbf{K}^{-1}(x,x')h(x')\right]\right\} \tag{B.4}$$

Where $\mathbf{K}^{-1}$ is defined by,

$$\int dx'\mathbf{K}(x,x')\mathbf{K}^{-1}(x',x'') = \delta(x-x''). \tag{B.5}$$

Ultimately, we don't need to worry about the constant of proportionality in equation B.4 because we'll be dividing this contribution when calculating correlation functions.

Appendix C

Binary Correlation Functions

When developing the binary PFC model we often change variables from ρ_A and ρ_B to n and c. This change of variable is helpful in identifying the results of the PFC theory with established results in the field as concentration and total density are more commonly used in the field of material science. Computing the bulk terms (ie., $\Delta\mathcal{F}_{mix}[n,c]$ and $\Delta\mathcal{F}_{id}[n]$ from equation 4.6 and 4.5) is a matter of substitution and simplification but computing the change of variables for excess free energy can be more subtle. When computing the pair correlation terms, careful application of our assumption that c varies over a much longer length scale than n must be applied to get the correct solution. The goal, ultimately, is to find C_{nn}, C_{nc}, C_{cn} and C_{cc} in the following expression,

[Stopped reviewing here! continue hhere in future]

$$\Delta\rho_A\,\rho_0 C_{AA} * \Delta\rho_A + \Delta\rho_A\,\rho_0 C_{AB} * \Delta\rho_B + \Delta\rho_B\,\rho_0 C_{BA} * \Delta\rho_A + \Delta\rho_B\,\rho_0 C_{BB} * \Delta\rho_B = \quad \text{(C.1)}$$
$$(n\,C_{nn} * n + n\,C_{nc} * \Delta c + \Delta c\,C_{cn} * n + \Delta c\,C_{cc} * \Delta c)\,.$$

We begin by rewriting $\Delta\rho_B$,

$$\begin{aligned}\Delta\rho_B &= \rho c - \rho_0 c_0 \\ &= \rho c - \rho c_0 + \rho c_0 - \rho_0 c_0 \\ &= \Delta\rho c + \rho_0 \Delta c,\end{aligned}$$

Followed by rewriting $\Delta\rho_A$,

$$\begin{aligned}\Delta\rho_A &= \rho(1-c) - \rho_0(1-c_0) \\ &= \Delta\rho(1-c) - \rho_0\Delta c.\end{aligned}$$

With those forms established, we can expand $\Delta\rho_B\, C_{BB} * \Delta\rho_B$:

$$\begin{aligned}\Delta\rho_B C_{BB} * \Delta\rho_B &= (\Delta\rho c + \rho_0\Delta c)\, C_{BB} * (\Delta\rho c + \rho_0\Delta c) \\ &= \Delta\rho c\, C_{BB} * (\Delta\rho c) \\ &+ \rho_0\Delta c\, C_{BB} * (\Delta\rho c) \\ &+ \rho_0\, (\Delta\rho c)\; C_{BB} * \Delta c \\ &+ \rho_0^2\Delta c\, C_{BB} * \Delta c.\end{aligned} \tag{C.2}$$

If we examine one term in this expansion in detail, we note that we can simplify by using the long wavelength approximation for the concentration field,

$$\begin{aligned}\Delta\rho c\, C_{BB} * \Delta\rho c &= \Delta\rho(r)c(r) \int dr' C_{BB}(r-r')\Delta\rho(r')c(r') \\ &\approx \Delta\rho(r)c^2(r) \int dr' C_{BB}(r-r')\Delta\rho(r').\end{aligned} \tag{C.3}$$

This is because the concentration field can be considered ostensibly constant over the length scale in which $C_{BB}(r)$ varies. Recall that the pair correlation function typically decays to

zero on the order of several particle radii. Using this approximation we can rewrite equation C.2 as,

$$\begin{aligned}\Delta\rho_B\, C_{BB} * \Delta\rho_B = {} & \Delta\rho \left(c^2\, C_{BB}\right) * \Delta\rho \\ & + \rho_0 \Delta c \left(c\, C_{BB}\right) * \Delta\rho c \\ & + \rho_0 \Delta\rho \left(c\, C_{BB}\right) * \Delta c \\ & + \rho_0^2 \Delta c\, C_{BB} * \Delta c.\end{aligned} \tag{C.4}$$

Repeating this procedure with the remaining three terms and then regrouping we can easily identify the required pair correlations.[1]

$$C_{nn} = \rho_0 \left(c^2\, C_{BB} + (1-c)^2\, C_{AA} + 2c(1-c)\, C_{AB}\right) \tag{C.5}$$

$$C_{nc} = C_{cn} = \rho_0 \left(c\, C_{BB} - (1-c)\, C_{AA} + (1-2c)\, C_{AB}\right) \tag{C.6}$$

$$C_{cc} = \rho_0 \left(C_{BB} + C_{AA} - 2C_{AB}\right) \tag{C.7}$$

[1]Note that we may also take advantage of the fact that $C_{AB} = C_{BA}$.

Bibliography

[1] Eli Alster, K. R. Elder, Jeffrey J. Hoyt, and Peter W. Voorhees. Phase-field-crystal model for ordered crystals. *Phys. Rev. E*, 95:022105, Feb 2017.

[2] Pep Español and Hartmut Löwen. Derivation of dynamical density functional theory using the projection operator technique. *The Journal of Chemical Physics*, 131(24):244101, 2009.

[3] Ronald Forrest Fox and George E. Uhlenbeck. Contributions to non-equilibrium thermodynamics. i. theory of hydrodynamical fluctuations. *Physics of Fluids*, 13(8):1893–1902, 1970.

[4] J. Willard Gibbs. *Elementary principles in statistical mechanics*. 1960.

[5] Michael Greenwood, Jörg Rottler, and Nikolas Provatas. Phase-field-crystal methodology for modeling of structural transformations. *Phys. Rev. E*, 83:031601, Mar 2011.

[6] Jean-Pierre Hansen and Ian R. McDonald. Appendix b: Two theorems in density functional theory. In Jean-Pierre Hansen and Ian R. McDonald, editors, *Theory of Simple Liquids (Fourth Edition)*, pages 587 – 589. Academic Press, Oxford, fourth edition edition, 2013.

[7] Jean-Pierre Hansen and Ian R. McDonald. Chapter 6 - inhomogeneous fluids. In Jean-Pierre Hansen and Ian R. McDonald, editors, *Theory of Simple Liquids (Fourth Edition)*, pages 203 – 264. Academic Press, Oxford, fourth edition edition, 2013.

[8] E. T. Jaynes. Information theory and statistical mechanics. *Phys. Rev.*, 106:620–630, May 1957.

[9] M. Kardar. *Statistical Physics of Fields*. June 2006.

[10] John G. Kirkwood. Quantum statistics of almost classical assemblies. *Phys. Rev.*, 44:31–37, Jul 1933.

[11] John G. Kirkwood and Elizabeth Monroe. Statistical mechanics of fusion. *The Journal of Chemical Physics*, 9(7):514–526, 1941.

[12] L.D. LANDAU and E.M. LIFSHITZ. Chapter iii - the gibbs distribution. In L.D. LANDAU and E.M. LIFSHITZ, editors, *Statistical Physics (Third Edition, Revised and Enlarged)*, pages 79 – 110. Butterworth-Heinemann, Oxford, third edition, revised and enlarged edition, 1980.

[13] Melvin Lax. Fluctuations from the nonequilibrium steady state. *Rev. Mod. Phys.*, 32:25–64, Jan 1960.

[14] Joseph E. Mayer and Elliott Montroll. Molecular distribution. *The Journal of Chemical Physics*, 9(1):2–16, 1941.

[15] Heather A. Murdoch and Christopher A. Schuh. Stability of binary nanocrystalline alloys against grain growth and phase separation. *Acta Materialia*, 61(6):2121 – 2132, 2013.

[16] L. Onsager and S. Machlup. Fluctuations and irreversible processes. *Phys. Rev.*, 91:1505–1512, Sep 1953.

[17] T. V. Ramakrishnan and M. Yussouff. First-principles order-parameter theory of freezing. *Phys. Rev. B*, 19:2775–2794, Mar 1979.

[18] David Ronis, Itamar Procaccia, and Jonathan Machta. Statistical mechanics of stationary states. vi. hydrodynamic fluctuation theory far from equilibrium. *Phys. Rev. A*, 22:714–724, Aug 1980.

[19] George E. Uhlenbeck and Erich Beth. The quantum theory of the non-ideal gas i. deviations from the classical theory. *Physica*, 3(8):729 – 745, 1936.

[20] E. Wigner. On the quantum correction for thermodynamic equilibrium. *Phys. Rev.*, 40:749–759, Jun 1932.